PROMOTING OF FOAM COPPER WITH CHAOTIC DISTRIBUTED PORES ON THE DEFLAGRATION OF PREMIXED HYDROGEN-AIR FLAME IN THE TUBE

Fengying LONG[1,2], Yulong DUAN[1,2*], Yunbing BU[1,2], Hailin JIA[3*], Shuwei YU[1,2], Jun HUANG[1,2]

1.College of Safety Engineering, Chongqing University of Science and Technology, Chongqing, 401331, China

2.Chongqing Key Laboratory for Oil and Gas Production Safety and Risk Control Technology, Chongqing, 401331, China

3.State Key Laboratory Cultivation Base for Gas Geology and Gas Control (Henan Polytechnic University), Jiaozuo, Henan 454003, China

*Corresponding author E-mail address: Yulong DUAN(2015014@cqust.edu.cn), Hailin JIA(jiahailin@126.com)

The deflagration flame of stoichiometric hydrogen-air mixtures is studied in this paper. Combined with the foam copper structure, the deflagration characteristic is analyzed in this paper. The experimental results show that the foam copper can improve the flow instability at the flame front and the degree of turbulence in the propagation process, the flame propagates more rapidly in turbulence state, and the number of stages of flame morphology during the propagation process increases. The classic "tulip" flame can be transformed into a distorted "tulip" flame and a fractal "tulip" flame before it collapses. When the flame passes through the foam copper, the flame front velocity increases as the number of structural layers increases. The flame front velocity propagates at supersonic speed through the accumulation of three layers of foam copper. The instability of overpressure in the propagation process will cause oscillation. More layers of the structure, the oscillation frequency, and the amplitude of the overpressure are increased significantly. Foam copper structure has a reverse action on overpressure. When the overpressure value is low in the early stage, the structure promotes the propagation, but the overpressure value is large in the later stage, the structure has a blocking effect.

Keywords: *foam copper; promote deflagration; instability; turbulence; overpressure oscillation*

1 Introduction

Hydrogen energy is regarded as clean energy with the most development potential in the 21st century. It has the characteristics of fast-burning rate, high laminar flame speed, and wide burning limit [1]. Hydrogen is a versatile energy carrier that can help meet a variety of energy challenges. The most basic way to use hydrogen is to make it react with combustion-supporting materials to produce heat, dynamic energy or to convert it into the form of energy needed by people. However, the

premixed deflagration flame is unstable when propagating in the pipeline and may be affected by different flow instability [2,3]. Therefore, people used many ways to understand and study the dynamic characteristics of the hydrogen deflagration/detonation process. When the premixed hydrogen-air is ignited, the flame is easily accelerated and can be converted into detonation under certain conditions [4].

The hazardous level will be seriously raised once there exists turbulence in the environment [5]. Joseph et al. [6] indicated that both local and global turbulent flame accelerations are improved once reactants with high turbulent intensity are inducted into the flame region and reacted at high turbulent combustion rates. The turbulent combustion rate will increase when the reactant mixture produces a heat diffusion unstable flame [7]. Xiao et al. [8,9] proved that flame instability play an important role in flame propagation. The instability of the flame and the interaction between the flame front wave and the pressure wave has positive feedback between the flame acceleration and turbulence generation.

When there are porous materials in the flame propagation path, the flame as a fluid medium will be profoundly affected by flow instability and pressure waves during the propagation process. The flame propagation process in the orifice is divided into laminar flames, jet flames and turbulent flames [10,11]. Wang et al. [12] proved that the instability and cellular structure of the hydrogen deflagration flame can cause the pressure to oscillate. The pressure behind the shock wave increases at the first, and then remains nearly constant with the increase of the propagation distance in the tube [13]. Ciccarelli [14] proved that there are many similarities between explosive propagation through porous media and channels full of obstacles, where flow obstacles in porous media can promote deflagration escalation. Ciccarelli et al. [15] further found that orifice plate spacing have a great effect on deflagration propagation velocity. The flame disturbance size in the hydrogen mixture increases with the increase of the pore size of the porous material of the channel wall [16]. Song et al. [17] proved that mesh aluminum alloys (playing roles as multiple obstacles) had a dual promoting/inhibiting effect on the deflagration of hydrogen-air mixtures. Johansen et al. [18] explained that the flame propagation in the porous layer is the reason for the flame acceleration in the channel. The smaller pore size of the porous media leads to more turbulence and more flame acceleration [19]. Jin et al. [20] proved that the single-layer metal wire mesh has a significant promotion effect on the formation time of the “tulip” flame, but the flame front reversal degree is weakened due to the weakening effect of the wire mesh on the flame front and the interaction of the pressure wave. Duan et al. [21] proved that large pore size porous materials can increase the flame propagation speed and accelerate the flame transition from layer to turbulence. Li et al. [22] proved that the sound waves generated between the orifice plates, after being reflected from the second plate, interact with the front part of the rear flame to produce a nearly flat flame. This phenomenon disappears with the shortening of the separation distance of the orifice plate. Although the evolution of flame shape under porous materials has been observed, the mechanism of flame behavior changes is not yet complete [23]. Babkin et al. [24] proved that the heat exchange between the flame and the porous material is limited, and the porous material can stretch the flame length or reduce the turbulent flame propagation speed.

The geometrical characteristics of porous materials are much more complex than obstacles, so there is no obvious transition state in the propagation process of deflagration flame, the propagation speed and pressure all change suddenly [21,25]. In summary, the previous research on porous materials mainly focused on evenly distributed orifice plates or non-metal porous materials. The performance characteristics of hydrogen explosion kinetics are stronger than that of alkane gases.

Besides, the inhibition effect of porous materials on the deflagration flame of alkanes forms a sharp contrast with the research in this paper [20]. Although there are many similarities between the effects of porous materials and obstacles on the deflagration propagation of combustible gases [14]. But the feedback mechanism of porous materials to the flame is more complicated. This paper takes the premixed hydrogen flame with an equivalent ratio of 1.0 as the research object, revealing the influence of foamed copper with randomly distributed pores on the explosion process.

2 Experimental details

As shown in Fig. 1, the experimental system includes the tube, the gas premixed system, the high-speed photographic system, the ignition system, and the high-frequency pressure acquisition system. The tube is made of plexiglass with a size of 500 × 100 × 100 mm^3. The gas premixed system consisted of a hydrogen cylinder (purity, 99.99%), an air cylinder, two gas mass flowmeters (ALICAT 20 accuracy 0.001 L/min), and many pneumatic accessories. The high-speed photographic system consisted of a high-speed camera and a high-performance computer. According to the size of the tube, the resolution of image acquisition is set as 1024×320, the Sample Rate is set as 10000 Hz. The high-frequency ignition system consists of a control switch, an ignition head, a transformer of AC to DC, a booster (input 15 V, output 500 V). The high-frequency pressure acquisition system consists of a pressure collector (Blast-PRO shock wave tester) and two high-frequency pressure sensors, which adopts the high-frequency ICP® pressure sensor (model, 113B28) produced by PCB Piezotronics.

The porous structure module in the experiment is realized by foam copper, and the size is 100×100×10 mm^3. The porosity of porous material is 20 PPI. The average pore size is about 2 mm. The layers of foam copper are 1, 2, and 3, as shown in Fig. 2. And foam copper has excellent sintering resistance and toughness, which is not easy to damage [26]. It has been used in much-advanced fire equipment, especially as flame isolation equipment, because of its good thermal conductivity and rapid dissipation of flame heat [27].

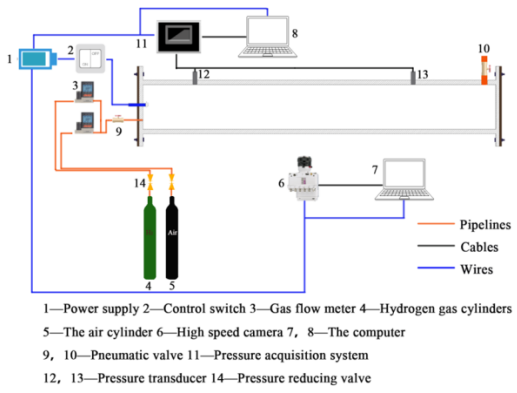

Fig. 1 Experimental system

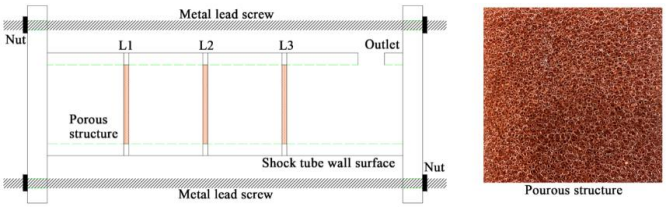

Fig. 2 Layout and detailed structure of foam copper

The stoichiometric ratio of the premixed hydrogen-air is 1.0. The components of the experimental system are installed and debugged following Fig. 1. The tube outlet is sealed with PVC film [25,28]. Previous studies have shown that PVC film only acts as safe pressure relief but has no effect on flame propagation in the tube [29,30]. The gas is mixed by two gas flowmeters, and finally fill into the tube to discharge the excess impurity gas, the four-fold volume exhaust method is adopted [31,32]. After the filled is over, the valves at both ends of the tube are closed, and the premixed gas in the tube is

allowed to stand for about 20 seconds to ensure the repeatability of the explosion experiment. The high-speed camera and pressure acquisition system are in the automatic trigger waiting state. The pressure and flame structure changes are collected and stored during the experiment. Each group of experiments is repeated 3 times at least to avoid experimental accidents and fluctuations in the collection system [33].

3 Results and discussion

3.1 Flame front structure changes

Fig. 3 shows Clanet et al. [34] testify four typical stages of deflagration flame propagation. (1) The initial state is the hemispherical flame propagating forward, $t_0<t<t_{sphere}$. The flame is restricted by the left wall and propagated in the hemispherical shape to the right. The flame instability is weak, and the flame mainly propagates in the laminar state [35] . There is an obvious and continuous boundary between the burned and the unburned at the flame front (t=1.8 ms). (2) The flame changes from the hemispherical to the finger-shaped, $t_{sphere}<t<t_{wall}$. The flame is affected by reflected waves from the wall. The flame is squeezed and stretched. The speed of the flame front increases rapidly. But the flame front still maintains a smooth shape (t=3.4~4.4 ms) and propagates with laminar. (3) The elongated flame skirt touches the tube wall, $t_{wall}<t<t_{tulip}$. The flame front speed starts to decrease due to the Rayleigh-Taylor instability, the flame front changes from finger-shaped to plane structure (t=7.0 ms). (4) The "tulip" flame stage, $t>t_{tulip}$. Currently, the flame front reverses, and the flame forms flame tongues near the wall, which are protruded forward obviously. When t=8.9 ms, the center of the flame front is sunken inward, and the "tulip" appears. Xiao et al. [36] proved the formation mechanism of the "tulip" flame, and proved that the difference in flame propagation speed eventually led to the formation of a distorted "tulip" flame. The interaction between the flow instability at the flame front and the pressure wave causes the flame to deform further, and the front angle gradually decreases from 111.22° to 62.45° (t=11.2 ms).

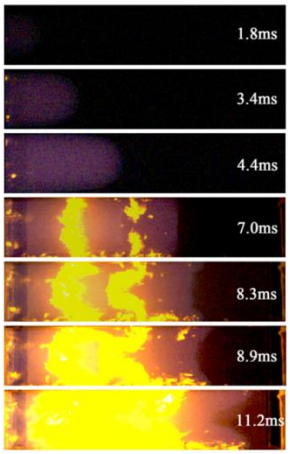

Fig. 3 Morphology of hydrogen-air deflagration flame at the corresponding position and moment of propagation in the tube

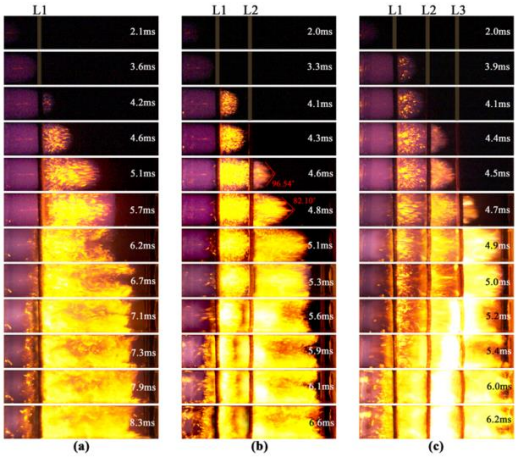

Fig. 4 Influence of foam copper on the propagation of deflagration flame (a) one layer (b) two layers (c) three layers

When porous structural are set in the tube, the hydrogen-air deflagration flame structure changed

with time as shown in Fig. 4. Fig. 4(a) shows the change of flame shape with one layer porous structure. It can be seen that *t*=2.1~3.6 ms, the flame forms the spherical shaped and finger shaped in the classic theory [34] as the flame front does not touch the foam copper. After the flame passes through the L1 structure (*t*=4.2 ms), then the L1 structure divides the flame into two regions. The flame propagates originally with a hemispherical shape in the downstream region. When *t*=4.6 ms, the flame develops rapidly in downstream after the flame passes through the L1. The chemical reaction inside the flame is intensified, and the flow of burned products is turbulent, but the flame front still maintained a regular finger shape. *t*=5.1 ms, the downstream flame skirt touches the inner wall, and the flame is squeezed by the wall and accelerates forward. The finger shape front is elongated until the flame front changed to plane at *t*=5.7 ms. At this moment, the flame front is strengthened by the influence of Rayleigh-Taylor instability, which forms the classic “tulip” (*t*=6.2 ms). The flame propagates from laminar flow to turbulence, and the internal chemical reaction is the largest [37]. The Rayleigh-Taylor instability caused by the pressure wave disturbing the flame destroys the regular shape of the flame front, and the obvious boundary between the burned and the unburned is broken. *t*= 6.7 ms, the classic "tulip" flame is distorted. The top flame tongue bends downward from the inner wall and the bottom flame tongue bends upward. The tip of the twisted "tulip" flame front begins to converge to the center [38]. *t*=7.1 ms, the top and bottom flame tongues of the distorted “tulip” flame gradually gather towards the center. During this period, the front of each flame tongue individual changed from protruding to indented, and the top and bottom flame tongues show the “tulip” shape respectively. This flame structure is defined as a fractal “tulip” flame because of the similarity between the part and the whole of the flame. Shen et al. [39] proved that the “tulip” distortion was conditional and substantially originates from the vibration just with more remarkable amplitude. The reason for this flame is that the Rayleigh-Taylor instability of the flame front increases greatly under the promotion of the reflected pressure wave. The flames changed into different shapes in the process of oscillating. *t*=7.3 ms, the distorted “tulip” flame front fuses to form a plane structure, and the flame near the wall extended to form flame tongues. The shape of the flame front is like Fig. 3 (*t*=8.3 ms). *t*=7.9~8.3 ms, the flame forms classic “tulip” again until dissipated. This result is mutually verified with Xiao et al.'s confirmation that the distorted “tulip” flame will form the classic “tulip” flame again until it collapsed [40]. After the flame passes through the L1 foam copper, it rapidly changes from laminar to turbulent. The evolution of flame shape experiences hemisphere→finger→plane→classic “tulip”→distorted “tulip”→fractal “tulip”→classic “tulip”.

Fig. 4(b) shows the change of hydrogen-air deflagration flame with two layers of porous structure in the tube. When the flame passes through the L1 structure, the interior of the hemispherical flame is disturbed more severely than with only one layer of foamed copper, *t*=4.1 ms. The boundary between the burned and the unburned is broken, and the flame fold clearly. The reason is that the foam copper promotes the flow, and when the flame propagates forward, it is simultaneously driven by its energy and drawn by the flow [31]. Therefore, the foam copper can promote the formation of instability propagation of hydrogen-air deflagration flame. *t*=4.3 ms, the radius of curvature of the flame front increases, and the flame has obvious burrs. The reason for the analysis is that the foam copper has a tearing effect on the original flame front, and the flame is divided into several small components after passing through the small channels, the flow stability and diffusion stability are destroyed. The collision probability of the free radicals in the channel is increased, and the flame accelerates at different speeds, so the original laminar smooth interface changes into an unstable cellular structure after passing through the porous structure. Meanwhile, the stretching degree of the flame front

increases. At *t*=4.6 ms, the flame develops rapidly in downstream, and the flame front propagates in a cone shape with the front angle of 96.54°. When *t*=4.8 ms, the center of the flame front is further stretched promoted by the disturbance of the L2 structure, and the front angle is 82.10°. *t*=5.1 ~ 5.3 ms, the flame changes from the finger shape to the plane *t*=5.6 ms, the classic “tulip” flame appears, and *t*=5.9 ms, the “tulip” flame tongues are stretched length. t=6.1 ms, the “tulip” appears on each flame tongue, then the fractal “tulip” flame appears, and reverts to the classic “tulip” at *t*=6.6 ms. The L2 structure further promotes the degree of turbulence after the flame front passes through L2. The flame front experienced the process finger→plane→classic “tulip”→distorted “tulip”→fractal “tulip”→classic “tulip”. Fig. 4(c) shows the influence of three layers of foam copper on the front structure of the deflagration flame. The propagation process of the flame through L1 and L2 is like Fig. 4(a) and Fig. 4(b). When *t*=4.7 ms, the flame front passes through the L3, and an irregular flame front appears in the downstream. The difference from the previous experimental results is that at *t*=6.0 ms, when the distorted “tulip” flame is closer to the right wall, the fractal “tulip” flame no longer appeared. The reason for this is that the reflected waves through the right wall are correspondingly higher due to the maximum facilitation of the pressure wave by L3. The tongues of the distorted "tulip" flames fuse together under the effect of flow instability and reflected pressure waves, but small "tulip" flames appear locally in front of the tongues. The result is a trident flame (two fused tulip flames). At *t*=6.2 ms, the tongues of the trident flames rolled again into their respective central parts until the flames filled the entire space. The three layers of foam copper, the flames appear as fingers → planes → classic "tulip" → distorted "tulip" → trident flame.

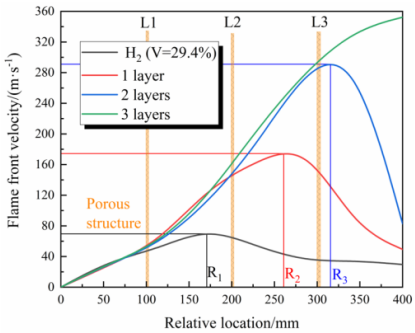

Fig. 5 The velocity of the flame front is affected by the layers of foam copper

3.2 Flame front propagation speed

The flame velocity is calculated according to the variation of the maximum axial distance of the flame front with time. Fig. 5 shows the velocity of the flame front during propagation. When the volume fraction of hydrogen is 29.4%, the flame front velocity reaches the maximum value of 69 m/s at the distance of R_1=168 mm from the ignition position. Then it drops to about 40 m/s at the distance of 275 mm from the ignition position and tends to be stable. When the foam copper place in the tube, the foam copper can increase the flame velocity. When the flame front passes through the L1, the velocity of the flame front increases rapidly and reaches the maximum value of 172 m/s at R_2=260 mm from the ignition position. Then it begins to decrease and tend to develop steadily. When there are two layers of foam copper in the tube, the velocity of the flame front is further increased when it passes through L2. The velocity of the flame front reaches the maximum value of 290 m/s at R_3=318 mm, and then begins to decrease. When three layers of foam copper are placed vertically in the tube, the flame front velocity increases similarly when passes through the L1 and L2. However, when the

flame passes through L3, the flame front velocity further increased and reached 353 m/s in the monitoring range, the flame propagates at supersonic (Mach number value is about 1.04). The flame front velocity is mainly derived from the fluid flow velocity[31], and maximum flame propagation velocity increased with the increase of pressure in the pipe[41]. So, the irregular pore structure of the foam copper can promote the interaction between overpressure and flame propagation velocity then accelerate the flame transition of laminar to turbulent. Previously, the foam copper can increase the flow effect, so that the protruding part of the flame front pushes more violently, and the propagation velocity of the flame front is increased. The turbulence degree and velocity of the flame are further intensified after passing through each layer of foam copper.

3.3 Deflagration overpressure changes with time

Fig. 6 shows the relationship between the overpressure and the time. The region between the ignition position and the foam copper defined as the upstream, and the region behind the foam copper defined as the downstream. Fig. 6(a) shows the overpressure of the upstream. The overpressure reaches the maximum value of 69.27 kPa at t_1^u =4 ms, and then propagates with a small range of oscillation around 53.0 kPa. The overpressure produces obvious oscillations during propagation when the foam copper is placed in the tube. The amplitude of overpressure oscillation also reflects the unstable combustion degree of premixed hydrogen-air. As shown in Fig. 6(a), when there is one layer of foam copper in the tube, the overpressure raises to 100.69 kPa (*t*=2.6 ms) and then briefly decreases. At t_2^u=2.9 ms, the pressure wave raises rapidly after descending to 97.0 kPa. The analysis reason is that the combustion reaction is fully reflected at this time, and the pressure wave generated is larger than that attenuation with the foam copper. In the subsequent time, the flame turbulence intensified after passing through the L1. The overpressure oscillates between 97.24 kPa and 177.51 kPa. The corresponding time of the maximum value of 177.51 kPa is *t*=4.7 ms. After t_3^u=7.2 ms, the overpressure oscillation phenomenon weakens and decreases gently. When the number of layers in the tube is increases, the overpressure oscillation phenomenon becomes more obvious, which is mainly manifested as an increase in the oscillation amplitude and frequency. The propagation of overpressure is promoted and attenuated at the same time, so, the maximum value of the overpressure and the slight decreasing trend at the initial stage are both increase. *t*=2.8 ms, the overpressure decreases after reaching 178.27 kPa in the upstream and raises sharply after reaching 153.08 kPa at t_4^u=3.2 ms, then appears the unstable propagation. There are four oscillation regions in the unstable propagation stage. t_5^u=5.8 ms, the overpressure declines gently. When the number of foam copper layers is increases again, the overpressure reaches 268.14 kPa at *t*=3.1 ms. When t_6^u=3.2 ms, the overpressure gradually began to rise after it decreased to 249.04 kPa. It enters the unstable propagation and reaches the maximum value of 383.65 kPa at *t*=3.4 ms. Compared with the two layers of foam copper, the three layers of foam copper shows four oscillation regions too in the unstable propagation stage, but the oscillation amplitude increases. However, the decline rate of the upstream overpressure increases with the increases of the number of porous layers. For the three layers of foam copper, the upstream overpressure declines at t_7^u=5.6 ms. When the layer of foam copper increases, the period of overpressure wave instability is shortened, the oscillation range is increased, and oscillation regions is increased. The overpressure propagation trend in the downstream is very different from that in the upstream (see Fig. 6(b)). When there was no foam copper in the tube, the overpressure value reaches

the maximum value of 88.69 kPa at t_1^d=4.9 ms. Compared with upstream, the overpressure increases and propagates stably at the maximum value without the downward trend. When the overpressure wave passes through L1, the rise rate increases rapidly after *t*=2 ms and propagates unsteadily at t_2^d= 2.4 ms. The overpressure reaches the maximum of 193.25 kPa at *t*=4.3 ms then decreases at t_3^d= 7.5 ms. When there are two layers of foam copper, the rise rate of overpressure increases at *t*=2 ms, then the overpressure increases again at *t*=2.4 ms and oscillates at t_4^d=2.6 ms. The overpressure reaches the maximum value of 321.44 kPa at *t*=2.9 ms during this period.t_5^d=5.5 ms, the overpressure begins to decline and ends the unstable propagation. When there are three layers of foam copper, the oscillation amplitude and frequency increase dramatically. After two accelerations, the overpressure raises sharply at t_6^d=2.7 ms and enters unstable propagation. The overpressure reaches the maximum value of 557.42 kPa at *t*=3.0 ms, and then oscillates around 300 kPa. *t*=5.3 ms, the oscillation propagation ends.

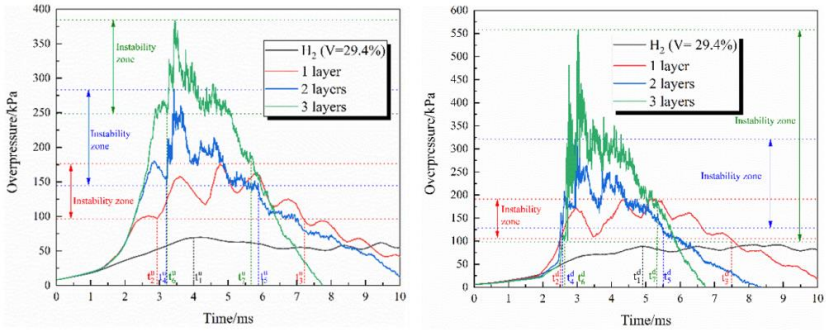

(a) The upstream (b) The downstream

Fig. 6 The trend of overpressure with time in the tube

Table 1 The corresponding periods and values of the various stages of overpressure (U: upstream D: downstream)

Foam copper layers	0		1		2		3	
	U	D	U	D	U	D	U	D
The initial moment of instability/ms	—	—	2.9	2.4	3.2	2.6	3.2	2.7
The end moment of instability/ms	—	—	7.2	7.5	5.8	5.5	5.6	5.3
Duration of instability /ms	—	—	4.3	5.1	2.6	2.9	2.4	2.6
The oscillation range of instability/kPa	—	—	97.24~177.51	109.41~193.25	153.08~282.27	131.11~321.44	249.04~383.65	101.20~557.42
The moment of maximum value/ms	4	4.9	4.7	4.3	3.3	2.9	3.2	3.0
The maximum value/kPa	69.27	88.69	177.51	193.25	282.27	321.44	383.65	557.42

It can be seen from Table 1 that the beginning of the unstable of overpressure in the downstream is less than that in the upstream. The duration of overpressure instability propagation decreases with

the increase of the number of layers of foam copper. The reason is that the increase of the layers can accelerate the propagation velocity of overpressure and flame in the tube, which decrease the deflagration reaction duration. The propagation time of the overpressure instability in the upstream is shorter than that in the downstream, then it is verified that the overpressure instability is generated in the downstream. However, when the layers increase, the oscillation range of overpressure increases significantly. When the number of layers is 1, 2 and 3, the oscillation amplitude of upstream overpressure is 80.27 kPa, 129.19 kPa and 134.61 kPa, the oscillation amplitude is 83.84 kPa, 190.33 kPa, 456.22 kPa in downstream. The overpressure in downstream is more violent. The difference between the oscillation amplitude of upstream and downstream is larger with the increase of layers. The downstream overpressure reaches the maximum value of 88.69 kPa at t=4.9 ms, which is larger than the upstream value, and the time is later. The difference of overpressure peak value between upstream and downstream is 15.74 kPa, 39.17 kPa and 173.77 kPa, it can be concluded that the strong turbulence of flame in downstream, leads to the unstable of overpressure and then spreads to the upstream. The propagation intensity of overpressure in downstream is greater than that in upstream, and the difference between the two regions is greater with the increase of layers. According to the upstream and downstream overpressure development, when the overpressure value is small, the porous structure can promote the spread of overpressure, but when the overpressure is large, the porous structure shows the effect of hindering propagation.

4 Conclusion

1) The foam copper can accelerate the propagation of hydrogen-air deflagration flame and accelerate the transition process of flame from laminar to turbulent, which makes the combustion reaction more intense and turbulence. After the flame front passes through the foamed copper, the influence of flow instability enhances, which increases the phase of flame deformations. The flame front shows the process finger → plane → classic "tulip"→distorted "tulip"→fractal "tulip"→classic "tulip". Three layers of foam copper can transform the flame into the trident.
2) The deflagration flame front velocity can be improved by the foam copper. The more layers, the more times the velocity is accelerated. Under some suitable conditions, the acceleration effect of porous materials on hydrogen flame is more obvious than obstacles. This is a content worth studying in the future.
3) After the overpressure passes through the foam copper, it propagates unsteadily in the downstream with oscillation. The amplitude and frequency of the oscillation increase with the increase of the foam copper layers. The foam copper can increase the peak value of overpressure. When the overpressure value is low, the foam copper promotes the overpressure evolution, but when the overpressure value is large, the porous structure has a blocking effect on the overpressure. The more layers of the foam copper, the greater the pressure difference between the upstream and downstream.

Acknowledgments

This work was supported by the Science and Technology Research Program of Chongqing

Municipal Education Commission (Grant No.KJQN202101503); The State Key Laboratory Cultivation Base for Gas Geology and Gas Control (Henan Polytechnic University)(WS2021A04); Open Foundation of the Chongqing Key Laboratory for Oil and Gas Production Safety and Risk Control(cqsrc202111); Graduate Science and Technology Innovation Project of Chongqing (CYS21503); Master's innovation program of Chongqing University of Science and Technology (YKJCX2020742).

Nomenclature

t	–time, [ms]	t_0	–initial time, [ms]
t_{sphere}	–the appearance time of spherical flame, [ms]	t_{wall}	–time when the flame first touches tube sidewalls, [ms]
t_{tulip}	–tulip flame occurrence time, [ms]	V	– hydrogen volume fraction, [%]
R	–distance from ignition position, [mm]	L	–layers of porous material
U	– upstream of porous material	D	–downstream of porous material

References

[1] Sánchez, A. L., et al., The chemistry involved in the third explosion limit of H2-O2 mixtures, *Combustion and Flame*, *161*(2014), 1, pp. 111–117. https://doi.org/10.1016/j.combustflame.2013.07.013.

[2] Ciccarelli G., Dorofeev S., Flame acceleration and transition to detonation in ducts, *Progress in Energy and Combustion Science*, *34*(2008), 4, pp. 499–550. https://doi.org/10.1016/j.pecs.2007.11.002.

[3] Najim Y. M., et al., On premixed flame propagation in a curved constant volume channel, *Combustion and Flame*, *162*(2015), 10, pp. 3980–3990. https://doi.org/10.1016/j.combustflame.2015.07.037.

[4] Dorofeev S. B., Evaluation of safety distances related to unconfined hydrogen explosions, *International Journal of Hydrogen Energy*, *32*(2007), 13,2118–2124. https://doi.org/10.1016/j.ijhydene.2007.04.003.

[5] Sun Z. Y., Experimental studies on the explosion indices in turbulent stoichiometric H2/CH4/air mixtures, *International Journal of Hydrogen Energy*, *44*(2019), 1, pp.469–476. https://doi.org/10.1016/j.ijhydene.2018.02.094.

[6] McGarry J. P., Ahmed K.A., Flame–turbulence interaction of laminar premixed deflagrated flames, *Combustion and Flame*, *176*(2017), pp. 439–450. https://doi.org/10.1016/j.combustflame.2016.11.002.

[7] Ahmed I., Swaminathan N., Simulation of turbulent explosion of hydrogen-air mixtures, *International Journal of Hydrogen Energy*, *39*(2014), 17, pp. 9562–9572. https://doi.org/10.1016/j.ijhydene.2014.03.246.

[8] Xiao H. H., et al., Effects of pressure waves on the stability of flames propagating in tubes, *Proceedings of the Combustion Institute*, *36*(2017), 1, 1577–1583. https://doi.org/10.1016/j.proci.2016.06.126.

[9] Xiao H. H., et al., Premixed flame propagation in hydrogen explosions, *Renewable and Sustainable Energy Reviews*, *81*(2018), 2, pp. 1988–2001.

https://doi.org/10.1016/j.rser.2017.06.008.
[10] Wei H. Q., et al., Different combustion modes caused by flame-shock interactions in a confined chamber with a perforated plate, *Combustion and Flame*, *178*(2017), pp. 277–285. https://doi.org/10.1016/j.combustflame.2017.01.011.
[11] Wei H. Q., et al., Effects of the equivalence ratio on turbulent flame–shock interactions in a confined space, *Combustion and Flame*, *186*(2017), 247–262. https://doi.org/10.1016/j.combustflame.2017.08.009
[12] Wang L.Q., et al., A comparative study of the explosion behaviors of H2 and C2H4 with air, N2O and O2, *Fire Safety Journal*, *119*(2021), pp.103260. https://doi.org/10.1016/j.firesaf.2020.103260.
[13] Duan Q. L., et al., Experimental study of shock wave propagation and its influence on the spontaneous ignition during high-pressure hydrogen release through a tube, *International Journal of Hydrogen Energy*, *44*(2019), 40, pp. 22598–22607. https://doi.org/10.1016/j.ijhydene.2019.06.166.
[14] Ciccarelli G., Explosion propagation in inert porous media, *Philosophical Transactions of the Royal Society A: Mathematical, Physical and Engineering Sciences*, *370*(2012), pp. 647–667. https://doi.org/10.1098/rsta.2011.0346.
[15] Ciccarelli G., et al., Effect of orifice plate spacing on detonation propagation, *Journal of Loss Prevention in the Process*, *49*(2017), pp. 739–44. https://doi.org/10.1016/j.jlp.2017.03.014.
[16] Golovastov S. V., et al., Influence of porous walls on flame front perturbations in hydrogen-air mixtures, *International Journal of Hydrogen Energy*, *46*(2021), 2, pp. 2783–2795. https://doi.org/10.1016/j.ijhydene.2020.10.028.
[17] Song X., et al., The explosion-suppression performance of mesh aluminum alloys and spherical nonmetallic materials on hydrogen-air mixtures, *International Journal of Hydrogen Energy*, *45*(2020), 56, pp. 32686–32701. https://doi.org/10.1016/j.ijhydene.2020.08.197.
[18] Johansen C., Ciccarelli G., Combustion in a horizontal channel partially filled with a porous media, *Shock Waves*, *18*(2008), pp. 97–106. https://doi.org/10.1007/s00193-008-0151-0.
[19] Liu F. S., et al., Experimental study on induced accelerated combustion of premixed hydrogen-air in a confined environment, *International Journal of Hydrogen Energy*, *44*(2019), 59, pp.31593–31609. https://doi.org/10.1016/j.ijhydene.2019.10.078.
[20] Jin K. Q., et al., Effect of single-layer wire mesh on premixed methane/air flame dynamics in a closed pipe, *International Journal of Hydrogen Energy*, *45*(2020), 56, pp. 32664–32675. https://doi.org/10.1016/j.ijhydene.2020.08.159.
[21] Duan Y. L., et al., Experimental study on methane explosion characteristics with different types of porous media, *Journal of Loss Prevention in the Process Industries*, *69*(2021) ,pp. 104370. https://doi.org/10.1016/j.jlp.2020.104370.
[22] Li Q., et al., Effect of orifice plates spaces on flame propagation in a square cross-section channel, *International Journal of Hydrogen Energy*, *44*(2019),40, pp. 22537–22546. https://doi.org/10.1016/j.ijhydene.2018.11.220.
[23] Jin K. Q., et al., Experimental study on the influence of multi-layer wire mesh on dynamics of premixed hydrogen-air flame propagation in a closed duct, *International Journal of Hydrogen Energy*, *42*(2017), 21, pp. 14809–14820. https://doi.org/10.1016/j.ijhydene.2017.03.232.
[24] Babkin V. S., et al., Propagation of premixed gaseous explosion flames in porous media, *Combustion and Flame*, *87*(1991), 2, pp. 182–90.

https://doi.org/10.1016/0010-2180(91)90168-B.
[25] Duan Y. L., et al., Experimental Study on Explosion of Premixed Methane-air with Different Porosity and Distance from Ignition Position, *Combustion Science and Technology*, *193*(2020), 12, pp. 2070-2084. https://doi.org/10.1080/00102202.2020.1727900.
[26] Sun J. H., et al., The comparative experimental study of the porous materials suppressing the gas explosion, *Procedia Engineering*, *26*(2011), pp. 954–960. https://doi.org/10.1016/j.proeng.2011.11.2262.
[27] Banhart J., Manufacture, characterisation and application of cellular metals and metal foams, *Progress in Materials Science*, *46*(2001), 6, pp. 559–632. https://doi.org/10.1016/S0079-6425(00)00002-5.
[28] Yu M. G., et al., Experimental study on explosion characteristics of syngas with different ignition positions and hydrogen fraction, *International Journal of Hydrogen Energy*, *44*(2019), 29, pp. 15553–15564. https://doi.org/10.1016/j.ijhydene.2019.04.046.
[29] Yang X. F., et al., A comparative investigation of premixed flame propagation behavior of syngas-air mixtures in closed and half-open ducts, *Energy*, *178*(2019), pp. 436–446. https://doi.org/10.1016/j.energy.2019.04.135.
[30] Wan S. J., et al., Effect of side vent size on a methane/air explosion in an end-vented duct containing an obstacle, *Experimental Thermal and Fluid Science*, *101*(2019), pp. 141–150. https://doi.org/10.1016/j.expthermflusci.2018.10.004.
[31] Duan Y. L., et al., Characteristics of gas explosion to diffusion combustion under porous materials (in Chinese), *Explosion and Shock Waves*, *40*(2020), 9, pp. 113–212. https://doi.org/10.11883/bzycj-2020-0009.
[32] Yu M. G., et al., Synergistic inhibition of gas explosion by ultrafine water mist-porous materials (in Chinese), *Journal of China Coal Society*, *44*(2019), 5, pp. 1562–1569. https://doi.org/10.13225/j.cnki.jccs.2018.0795.
[33] Wang T., et al., The explosion enhancement of methane-air mixtures by ethylene in a confined chamber, *Energy*, *214*(2021), pp. 119042. https://doi.org/10.1016/j.energy.2020.119042.
[34] Clanet C., Searby G., On the "Tulip flame" phenomenon, *Combustion and Flame*, *105*(1996), 1-2, pp. 225–38. https://doi.org/10.1016/0010-2180(95)00195-6.
[35] Qin Y., Chen X. W., Flame propagation of premixed hydrogen-air explosion in a closed duct with obstacles, *International Journal of Hydrogen Energy*, *46*(2021), 2, pp. 2684–701. https://doi.org/10.1016/j.ijhydene.2020.10.097.
[36] Xiao H. H., et al., Experimental study on the behaviors and shape changes of premixed hydrogen-air flames propagating in horizontal duct, *International Journal of Hydrogen Energy*, *36*(2011), 10, pp. 6325–36. https://doi.org/10.1016/j.ijhydene.2011.02.049.
[37] Zheng K., et al., Effects of hydrogen addition on methane-air deflagration in obstructed chamber, *Experimental Thermal and Fluid Science*, *80*(2017), pp. 270–80. https://doi.org/10.1016/j.expthermflusci.2016.08.025.
[38] Xiao H. H., et al., Formation and evolution of distorted tulip flames, *Combustion and Flame*, *162*(2015), 11, pp. 4084–101. https://doi.org/10.1016/j.combustflame.2015.08.020.
[39] Shen X. B., et al., Experimental study on the characteristic stages of premixed hydrogen-air flame propagation in a horizontal rectangular closed duct, *International Journal of Hydrogen Energy*, *37*(2012), 16, pp. 12028–12038. https://doi.org/10.1016/j.ijhydene.2012.05.084.
[40] Xiao H. H., et al., Experimental and numerical study of premixed hydrogen/air flame

propagating in a combustion chamber, *Journal of Hazardous Materials*, *268*(2014), pp. 132–139. https://doi.org/10.1016/j.jhazmat.2013.12.060.

[41] Wang C., et al., Experimental investigation on explosion flame propagation of H2-O2 in a small scale pipeline, *Journal of Loss Prevention in the Process Industries*, *49*(2017), 612–619. https://doi.org/10.1016/j.jlp.2017.06.004

Paper submitted: 05.04.2022
Paper revised: 28.04.2022
Paper accepted: 06.05.2022